JACS
JOURNAL OF THE AMERICAN CHEMICAL SOCIETY
Communication
pubs.acs.org/JACS

Selective Scission of C−O and C−C Bonds in Ethanol Using Bimetal Catalysts for the Preferential Growth of Semiconducting SWNT Arrays

Shuchen Zhang, Yue Hu, Juanxia Wu, Dan Liu, Lixing Kang, Qiuchen Zhao, and Jin Zhang*

Center for Nanochemistry, Beijing National Laboratory for Molecular Sciences, Key Laboratory for the Physics and Chemistry of Nanodevices, State Key Laboratory for Structural Chemistry of Unstable and Stable Species, College of Chemistry and Molecular Engineering, Peking University, Beijing 100871, P. R. China

Supporting Information

ABSTRACT: For the application of single-walled carbon nanotubes (SWNTs) to electronic and optoelectronic devices, techniques to obtain semiconducting SWNT (s-SWNT) arrays are still in their infancy. We have developed herein a rational approach for the preferential growth of horizontally aligned s-SWNT arrays on a ST-cut quartz surface through the selective scission of C−O and C−C bonds of ethanol using bimetal catalysts, such as Cu/Ru, Cu/Pd, and Au/Pd. For a common carbon source, ethanol, a reforming reaction occurs on Cu or Au upon C−C bond breakage and produces C_{ads} and CO, while a deoxygenating reaction occurs on Ru or Pd through C−O bond breaking resulting in the production of O_{ads} and C_2H_4. The produced C_2H_4 by Ru or Pd can weaken the oxidative environment through decomposition and the neutralization of O_{ads}. When the bimetal catalysts with an appropriate ratio were used, the produced C_{ads} and C_2H_4 can be used as carbon source for SWNT growth, and O_{ads} promotes a suitable and durable oxidative environment to inhibit the formation of metallic SWNTs (m-SWNTs). Finally, we successfully obtained horizontally aligned SWNTs on a ST-cut quartz surface with a density of 4−8 tubes/μm and an s-SWNT ratio of about 93% using an Au/Pd (1:1) catalyst. The synergistic effects in bimetallic catalysts provide a new mechanism to control the growth of s-SWNTs.

The application of single-walled carbon nanotubes (SWNTs) to nanoelectronic devices[1−4] is prevented by the fact that almost all of the currently available technologies only produce a mixture of metallic (m-) and semiconducting (s-) SWNTs. This coexistence of as-grown samples dramatically decreases device performance. Many groups have devoted time to developing the different methods of obtaining s-SWNTs. However, the selective production of s-SWNTs, especially s-SWNTs arrays on a surface, is still a challenge.

Over the past two decades, several approaches have been developed for the production of s-SWNT arrays including direct chemical vapor deposition (CVD) growth and post-treatment approaches. In the case of post-treatment approaches, etching methods have proved to be an efficient way to obtain a SWNT array containing more than 95% s-SWNTs by the introduction of methane plasma,[5] SO_3,[6] and electromagnetic radiation.[7] However, these methods decrease the density of the s-SWNT array significantly. SDS washing,[8] scotch tape separation,[9] and electrophoresis[10] inevitably also decrease the density and introduce contamination, and thus, these materials cannot be used in high performance devices. These shortcomings severely limit the performance of SWNT-based devices. The direct growth method, with the introduction of oxidative gases and an external field such as water,[11] oxygen,[12] and UV light,[13] is a better method to preferentially grow an s-SWNT array.

In the CVD system, the carbon sources selection[14,15] and the catalyst design[16−18] are important for the optimum growth of s-SWNT arrays. Many single metals and their alloys such as Fe/Cu[17] and Fe/Ru[16] have been found to favor the growth of random semiconducting SWNTs with an unknown mechanism. Ethanol, as a common carbon source, can be decomposed in different pathways when using different catalysts.[19] Reforming reaction 1 occurs through selective C−C and C−H bond scission to produce C_{ads} and CO. Deoxygenation reaction 2 is selective toward C−O bond cleavage to produce O_{ads} and C_2H_4.

$$C_2H_5OH \rightarrow CO + C_{ads} + 3H_2 \quad (1)$$

$$C_2H_5OH \rightarrow C_2H_4 + O_{ads} + H_2 \quad (2)$$

The dominant ethanol reaction pathway can be controlled by deoxygenation on Ru[20] and reforming on Cu.[19] In our work, we used bimetal catalysts consisting of Ru and Cu for the preferential growth of s-SWNTs. The as-produced O_{ads} when using Ru resulted in a feasible oxidative environment to ensure the reliable elimination of m-SWNTs, and this led to s-SWNTs of high purity. Cu provided C_{ads} for the growth of SWNTs during the tube's growth process. Other bimetal catalysts such as Au/Ru, Au/Pd, and Cu/Pd were also used to grow s-SWNT arrays because of similar properties. We successfully obtained horizontally aligned SWNTs on a ST-cut quartz surface with a density of 4−8 tubes/μm and a s-SWNT ratio of about 93% using Au/Pd (1:1) catalyst. Raman spectra and electrical measurements indicated that the SWNTs grown using this method were semiconducting tubes.

During SWNT growth we intended to use the O_{ads} produced by Ru through the scission of C−O in ethanol to maintain an oxidative environment to inhibit the formation of m-SWNTs. Bimetal catalysts were thus developed to preferentially grow

Received: October 22, 2014
Published: January 13, 2015

DOI: 10.1021/ja510845j
J. Am. Chem. Soc. 2015, 137, 1012−1015

horizontally aligned s-SWNTs. Figure 1a schematically shows the design of the bimetal catalysts that were used to grow the s-

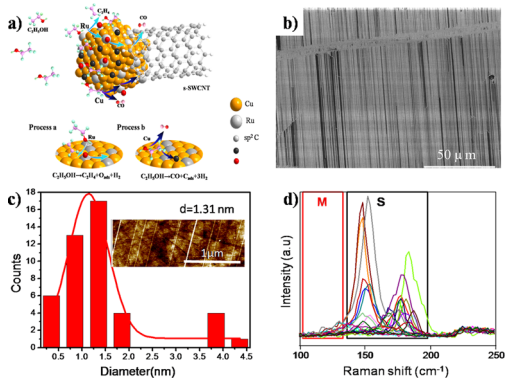

Figure 1. (a) Scheme showing the mechanism of s-SWNTs growth when using bimetal catalysts. (b) SEM of the SWNTs synthesized using Cu/Ru (3:1) catalyst. (c) Distribution of the as-grown SWNTs is 1.31 nm, and the inset is an AFM of the SWNTs. (d) Raman spectra of the SWNTs array measured using 514 nm laser.

SWNTs array. Cu and Ru were selected with the ratio of 3:1 because the reforming reaction occurs on Cu and the deoxygenation reaction occurs on Ru. The bimetal catalyst was obtained by reducing precursors of a mixed solution that was added dropwise onto ST-cut quartz substrates (details in the methods section, SI). Figure 1b gives scanning electron microscopy (SEM) results for the SWNTs obtained using the bimetal Cu/Ru (3:1) catalyst. This shows that the as-grown SWNTs have a large area and are uniform with perfect alignment, and the average density was found to be at least 5 tubes/μm. Furthermore, the inset AFM in Figure 1c confirms this measurement.

To determine the difference between the SWNTs obtained using different catalysts, the single metals catalysts, Cu and Ru, were also used to grow SWNTs under the same conditions. The results are shown in Figure S1a ,b. Well-aligned SWNTs were obtained for both the Cu and Ru catalysts. AFM images in Figure S1c,d confirmed the densities of the SWNTs were 6 and 8 tubes/μm for Cu and Ru, respectively. Compared with the density of the SWNT array prepared using Cu/Ru (3:1), no significant difference was observed. However, a difference in diameter distribution was observed in three different catalysts. Figure 1c shows a diameter analysis of the tubes prepared using Cu/Ru (3:1) and a narrow distribution of 1.3 $\pm$ 0.3 nm. A wide distribution of SWNT diameters was found for Cu and Ru as shown in Figure S1e,f.

Raman spectroscopy with excitation by laser at 514 and 633 nm, combined with electrical measurements, was used to characterize the structure and electronic properties of the as-grown SWNT arrays.[21] Figure 1d and Figure 2a give typical radial breathing mode (RBM) peaks from Raman spectra of the SWNT samples prepared as Cu/Ru (3:1) with 514 and 633 nm excitation. m-SWNTs were hardly detected for the SWNTs grown using Cu/Ru (3:1). However, for the monometallic catalysts, Cu and Ru, the RBMs were randomly distributed as shown in Figures 2b,c and S2a,b. Figure 2d shows statistics for the m-SWNTs and s-SWNTs prepared using different catalysts. The abundance of s-SWNTs was ~91% for the samples synthesized using the Cu/Ru catalyst by comparison with ~78% for the Cu catalyst and ~80% for the Ru catalyst. To further verify the high ratio of s-SWNTs in these samples, we

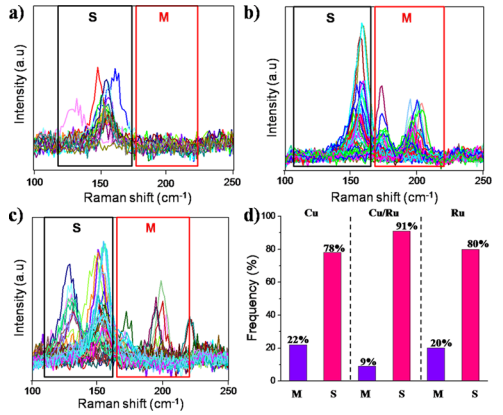

Figure 2. Raman spectra of the SWNTs obtained using different catalysts, (a) Cu/Ru (3:1), (b) Ru, and (c) Cu, measured using a 633 nm laser. (d) Statistics of the m-SWNTs (denoted M) and the s-SWNTs (denoted S) obtained using different catalysts and measured using 514 and 633 nm lasers.

carried out electrical measurements in field effect transistors (FET). Details of the fabrication and test processes of the FET devices are described in the methods section. $I-V$ curves are shown in Figure S2c, and the on/off ratio was 10.9, which indicates typical semiconducting behavior for the channel materials. We carefully compared the G bands of the SWNTs grown using the monometallic and bimetal catalysts. From Figure S3, the SWNTs from Cu/Ru do not show a BWF band, while the SWNTs grown using Cu or Ru sometimes show obvious BWF bands, which is a typical characteristic of m-SWNTs.

To thoroughly study the relationship between selectivity and the bimetal catalyst, we explored the dependence of selectivity on the Cu and Ru ratios of the catalysts. Cu/Ru with ratios of 1:3 and 1:1 were considered. Both these bimetal catalysts were successfully applied to the growth of a SWNT array. SEM results for the two catalysts, Cu/Ru (1:3) and Cu/Ru (1:1), are shown in Figure S4a,b respectively. We found that m-SWNTs of different ratios were formed when using bimetal catalysts at the 1:3 (Figures 3a and S4c) and 1:1 (Figures 3b and S4d) ratios. To compare the results, a statistical analysis of the m-SWNTs and s-SWNTs obtained using the different catalysts are shown in Figure 3c. We found 84% s-SWNTs for Cu/Ru (1:3) and 88% for Cu/Ru (1:1). An interesting phenomenon was also observed. With a decrease of Ru in the bimetal catalysts, the ratio of the s-SWNTs increased. Therefore, small amounts of Ru mixed with the Cu catalyst to improve selectivity toward s-SWNTs. Higher amounts of Ru in the bimetal catalysts result in an increase in the deoxygenation reaction giving more C_2H_4. Ethylene, at 800 °C, which is usually used for tube growth, easily is decomposed into C free radicals. The extra C will weaken the oxidative environment created by O_{ads} by neutralization. Selectivity toward s-SWNTs thus decreases.

To prove our hypothesis about the s-SWNT array being governed by the selective scission of C−O and C−C bonds in ethanol we characterized the bimetal catalysts. X-ray photoelectron spectroscopy (XPS) was used to detect the valence state of Cu in the bimetal catalyst. As shown in Figure S5, two states of Cu exist in the catalysts, Cu^0 (932.7 eV) and Cu^{2+} (933.7 eV). Cu^{2+} can be attributed to existing CuO, which is formed upon oxidation in air before detection by XPS. No indication was found that an interaction exists between reduced Cu and Ru. The phase diagram of Cu and Ru also shows their immiscibility

DOI: 10.1021/ja510845j
J. Am. Chem. Soc. 2015, 137, 1012−1015

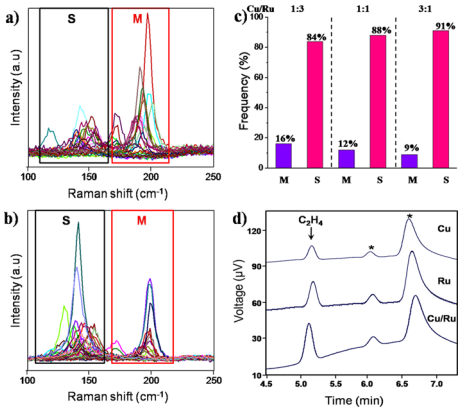

Figure 3. Raman spectra of the SWNTs obtained using Cu/Ru catalysts with different ratios, (a) 1:3 and (b) 1:1, measured with a 633 nm laser. (c) Statistics for the m-SWNTs (denoted M) and the s-SWNTs (denoted S) obtained using different catalysts and measured using 514 and 633 nm lasers. (d) GC analysis of the exhaust mixtures, especially C_2H_4 with a retention time of 5.21 min in this system, collected during the growth of the SWNTs. *Represents unknown species that were produced during the growth of the SWNTs.

because of a weak interaction independent of the phase being solid or liquid. Therefore, during tube growth, independent catalytic behavior is evident when decomposing ethanol.

Gas chromatography (GC)[22] was used to analyze the reforming reaction and the deoxygenation reaction that occurred on the catalysts. GC can be used to separate and analyze C_2H_4 and CO from the exhaust mixture, which mainly contains Ar and H_2, using retention time. Exhaust gases were collected during the growth processes when using the Ru, Cu, and Cu/Ru (1:1) catalysts. The analysis results were compared after normalizing based on the peak area of argon, and the results are shown in Figure 3d. We found that far more C_2H_4 was present in the gas mixtures produced by Ru, and a few was found for the Cu catalyst under the same conditions. The ethylene present in the Cu system was produced by thermal decomposition at high temperature. Through GS analysis, the decompositions of ethanol over the different catalysts were found to be different because of deoxygenation on Ru and reforming on Cu. Figure S6a shows that a similar amount of CO was detected for all three catalysts because the O in ethanol will always transfer to CO.

To better understand the important role of the deoxygenation reaction on Ru on the selectivity of s-SWNTs, we varied the flow rate of hydrogen and argon (using an ethanol bubbler). This was done to obtain a relationship between the selectivity and the C/H ratio. The results are shown in Figure S6b. At a high C/H ratio, the possibility of ethanol absorbing on Ru increases, and this leads to more C_2H_4 being produced by deoxygenation. C_2H_4 can weaken the oxidative environment. The semiconducting SWNT selectivity disappears. Therefore, the selectivity toward s-SWNT is improved at a lower C/H ratio.

To rule out other possibilities playing an important role in s-SWNT selectivity and to distinguish the effect of oxygen in ethanol, a carbon source without oxygen such as CH_4 can be used to grow SWNTs. We used the Cu/Ru (3:1) catalyst for this test. The results are shown in Figure S7. Many m-SWNTs appeared, indicating that the selectivity does indeed originate from the oxygen in ethanol. Understanding the behaviors of the different catalysts, single metals, or bimetals may provide insights into the mechanism of SWNTs growth and how to control it at high temperature.

Furthermore, this approach was developed using other bimetal catalysts (i.e., Cu/Pd, Au/Ru, and Au/Pd) for the growth of an s-SWNT array because Cu and Au, as well as Ru and Pd, have similar properties, respectively. The results are shown in Figure S8. A Raman spectrum was used to characterize the SWNTs, and the results are given in Figure S9. We varied the composition of the catalysts and a similar relationship between the ratios of the different metals in bimetal catalysts, and their selectivity toward SWNTs was found for the different bimetal catalysts as shown in Figure S10.

Finally, we fabricated several back-gated SWNT array FETs using Au/Pd (1:1) catalyzed s-SWNT enriched samples, and they showed higher selectivity compared with the other bimetal catalyzed samples. They were transferred from a ST-cut quartz substrate to heavily doped silicon substrates (~300 nm insulating silica layer). Figure 4a shows SEM images of the devices. A FET

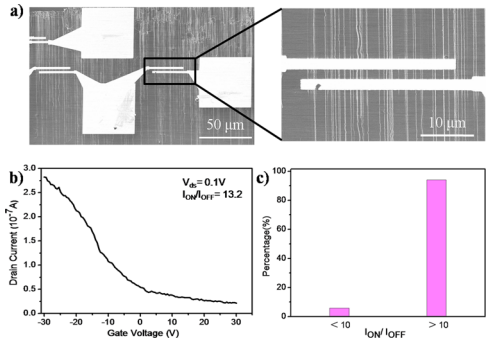

Figure 4. (a) SEM images of the FET devices fabricated on the as-grown SWNT arrays using Au/Pd (1:1) as the catalysts transferred onto the SiO_2/Si substrate. (b) Typical transfer characteristic curve for the s-SWNT device with V_{dss} = 100 mV. (c) Statistical result of the I_{on}/I_{off} ratio of the devices.

typically contained several nanotubes. The $I-V$ curves shown in Figure 4b reveal typical semiconducting behavior for the channel materials, that is, the SWNTs. The semiconducting tube content of this device was estimated to be about 93%. More FETs and $I-V$ curves of the FETs are shown in Figure S11. The estimated contents of s-SWNTs for these devices are all higher than 91%, which is consistent with the ratio obtained by Raman measurements.

In conclusion, we found that Ru and Cu behave differently as catalysts for the growth of SWNTs through the decomposing ethanol, and they can be used to catalyze the synthesis of s-SWNT arrays in a synergistic manner. A reasonable mechanism is suggested. O_{ads} can be produced on Ru, and it will migrate on the surface of catalysts to create oxidation conditions. Therefore, m-SWNT production is impeded, and a s-SWNT array is preferred. Because the added metal plays an important role in the generating oxygen and a balance exists between the etching and growth of SWNTs, it is reasonable to expect more flexibility in this strategy when choosing the two metals. Alternative experiments, using metals such as Au or Pd, were conducted to confirm this. The growth of SWNTs using bimetal catalysts provides a new understanding about the mechanism of catalytic SWNT formation. Finally, the FETs fabricated using the samples produced confirm that the SWNT array has high s-SWNT selectivity when using bimetal catalysts.

DOI: 10.1021/ja510845j
J. Am. Chem. Soc. 2015, 137, 1012−1015

■ ASSOCIATED CONTENT

Supporting Information

Experimental details, detail Raman spectrum analysis data, SEM images, AFM images, GS data, FET devices. This material is available free of charge via the Internet at http://pubs.acs.org.

■ AUTHOR INFORMATION

Corresponding Author

*jinzhang@pku.edu.cn

Notes

The authors declare no competing financial interest.

■ ACKNOWLEDGMENTS

This work was supported by NSFC (21233001, 21129001, 51272006, 51432002, and 51121091) and MOST (2011CB932601).

■ REFERENCES

(1) Shulaker, M. M.; Hills, G.; Patil, N.; Wei, H.; Chen, H. Y.; PhilipWong, H. S.; Mitra, S. *Nature* **2013**, *501*, 526.

(2) Shulaker, M. M.; Van Rethy, J.; Wu, T. F.; Liyanage, L. S.; Wei, H.; Li, Z. Y.; Pop, E.; Gielen, G.; Wong, H. S. P.; Mitra, S. *ACS Nano* **2014**, *8*, 3434.

(3) Cao, Q.; Han, S. J.; Tulevski, G. S. *Nat. Commun.* **2014**, *5*, 5071.

(4) Chen, Y.; Zhang, J. *Acc. Chem. Res.* **2014**, *47*, 2273.

(5) Li, Y. M.; Mann, D.; Rolandi, M.; Kim, W.; Ural, A.; Hung, S.; Javey, A.; Cao, J.; Wang, D. W.; Yenilmez, E.; Wang, Q.; Gibbons, J. F.; Nishi, Y.; Dai, H. J. *Nano Lett.* **2004**, *4*, 317.

(6) Yang, C. M.; An, K. H.; Park, J. S.; Park, K. A.; Lim, S. C.; Cho, S. H.; Lee, Y. S.; Park, W.; Park, C. Y.; Lee, Y. H. *Phys. Rev. B* **2006**, *73*, 075419.

(7) Huang, H. J.; Maruyama, R.; Noda, K.; Kajiura, H.; Kadono, K. *J. Phys. Chem. B* **2006**, *110*, 7316.

(8) Hu, Y.; Chen, Y.; Li, P.; Zhang, J. *Small* **2013**, *9*, 1306.

(9) Hong, G.; Zhou, M.; Zhang, R. O. X.; Hou, S. M.; Choi, W.; Woo, Y. S.; Choi, J. Y.; Liu, Z. F.; Zhang, J. *Angew. Chem., Int. Ed.* **2011**, *50*, 6819.

(10) Cao, Q.; Han, S. J.; Tulevski, G. S.; Zhu, Y.; Lu, D. D.; Haensch, W. *Nat. Nanotechnol.* **2013**, *8*, 180.

(11) Zhou, W. W.; Zhan, S. T.; Ding, L.; Liu, J. *J. Am. Chem. Soc.* **2012**, *134*, 14019.

(12) Yu, B.; Liu, C.; Hou, P. X.; Tian, Y.; Li, S. S.; Liu, B. L.; Li, F.; Kauppinen, E. I.; Cheng, H. M. *J. Am. Chem. Soc.* **2011**, *133*, 5232.

(13) Zhang, Y. Y.; Zhang, Y.; Xian, X. J.; Zhang, J.; Liu, Z. F. *J. Phys. Chem. C* **2008**, *112*, 3849.

(14) Ding, L.; Tselev, A.; Wang, J. Y.; Yuan, D. N.; Chu, H. B.; McNicholas, T. P.; Li, Y.; Liu, J. *Nano Lett.* **2009**, *9*, 800.

(15) Feng, X. F.; Chee, S. W.; Sharma, R.; Liu, K.; Xie, X.; Li, Q. Q.; Fan, S. S.; Jiang, K. L. *Nano Res.* **2011**, *4*, 767.

(16) Li, X. L.; Tu, X. M.; Zaric, S.; Welsher, K.; Seo, W. S.; Zhao, W.; Dai, H. J. *J. Am. Chem. Soc.* **2007**, *129*, 15770.

(17) He, M.; Chernov, A. I.; Fedotov, P. V.; Obraztsova, E. D.; Sainio, J.; Rikkinen, E.; Jiang, H.; Zhu, Z.; Tian, Y.; Kauppinen, E. I.; Niemela, M.; Krauset, A. O. I. *J. Am. Chem. Soc.* **2010**, *132*, 13994.

(18) Yang, F.; Wang, X.; Zhang, D.; Yang, J.; Luo, D.; Xu, Z.; Wei, J.; Wang, J.-Q.; Xu, Z.; Peng, F.; Li, X.; Li, R.; Li, Y.; Li, M.; Bai, X.; Ding, F.; Li, Y. *Nature* **2014**, *510*, 522.

(19) Kelly, T. G.; Chen, J. G. *ACS Symp. Ser.* **2014**, *16*, 777.

(20) Williams, R. M.; Pang, S. H.; Medlin, J. W. *Surf. Sci.* **2014**, *619*, 114.

(21) Soares, J. S.; Cancado, L. G.; Barros, E. B.; Jorio, A. *Phys. Status Solidi B* **2010**, *247*, 2835.

(22) Jalbert, J.; Gilbert, R.; Tetreault, P. *Anal. Chem.* **2001**, *73*, 3382.

DOI: 10.1021/ja510845j
J. Am. Chem. Soc. 2015, 137, 1012−1015